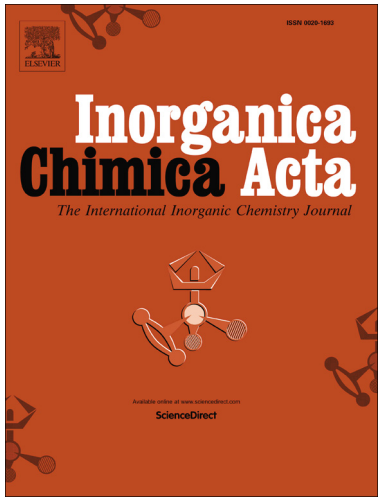

Research paper

Synthesis and Characterization of *N,N',C*-bound Organotellurium(IV) and Organomercury(II) Derivatives

Puspendra Singh, Anand K. Gupta, Sagar Sharma, Harkesh B. Singh, Ray J. Butcher

PII: S0020-1693(18)30680-7
DOI: https://doi.org/10.1016/j.ica.2018.08.016
Reference: ICA 18416

To appear in: *Inorganica Chimica Acta*

Received Date: 4 May 2018
Revised Date: 14 August 2018
Accepted Date: 14 August 2018

Please cite this article as: P. Singh, A.K. Gupta, S. Sharma, H.B. Singh, R.J. Butcher, Synthesis and Characterization of *N,N',C*-bound Organotellurium(IV) and Organomercury(II) Derivatives, *Inorganica Chimica Acta* (2018), doi: https://doi.org/10.1016/j.ica.2018.08.016

Synthesis and Characterization of *N,N',C*-bound Organotellurium(IV) and Organomercury(II) Derivatives

Puspendra Singh[a,b], Anand K. Gupta[a], Sagar Sharma[c], Harkesh B. Singh[a,*], Ray J. Butcher[d]

[a]*Department of Chemistry, Indian Institute of Technology Bombay, Mumbai 400076, India*

[b]*Department of Chemistry, Dr. Shakuntala Misra National Rehabilitation University Lucknow, Uttar Pradesh, 226017, India*

[c]*Physical Sciences Division, Institute of Advanced Study in Science & Technology, Paschim Boragaon, Guwahati-781035, Assam, India*

[d]*Department of Chemistry, Howard University, Washington DC20059, USA*

Abstract

We report the synthesis and characterization of the first examples of organotellurium (IV)/organomercury(II) derivatives of *N,N',C*-chelating aryldiamine ligand, 2-{$Me_2NCH_2CH_2N(Me)CH_2$}C_6H_4Br (**20**). The dichalcogenides, [2-{$Me_2NCH_2CH_2N(Me)CH_2$}$C_6H_4Se]_2$ (**24**) and [2-{$Me_2NCH_2CH_2N(Me)CH_2$}$C_6H_4Te]_2$ (**25**), were prepared by treatment of the corresponding Grignard reagent (**21**)/organolithium reagent (**22**) in THF with selenium or tellurium, respectively. Compounds [2-{$Me_2NCH_2CH_2N(Me)CH_2$}$C_6H_4]_2Se$ (**26**) and [2-

{$Me_2NCH_2CH_2N(Me)CH_2$}C_6H_4]Te($S_2CN(CH_2CH_3)_2$ (**27**) were synthesized by the reaction of **21**/**22** with $Se(dtc)_2$ in 2:1 or $Te(dtc)_2$ (dtc = diethyldithiacarbamate) in 1:1 ratio at room temperature. In contrast, the reaction of **21** with TeI_2 afforded an unexpected protonated derivative, [2-{(Me_2NH)$CH_2CH_2N(Me)CH_2$}$C_6H_4TeI]^+(I)^-$ (**28a**). Similarly, the halogenation reactions of **25** with chlorine gas or a solution of bromine in THF afforded protonated derivatives, [2-{(Me_2NH)$CH_2CH_2N(Me)CH_2$}$C_6H_4TeCl_3]^+(Cl)^-$ (**29a**) and [2-{(Me_2NH)$CH_2CH_2N(Me)CH_2$}$C_6H_4TeBr_3]^+(Br)^-$ (**30a**), respectively. The organomercury precursors; 2-{$Me_2NCH_2CH_2N(Me)CH_2$}$C_6H_4HgCl_{0.54}/Br_{0.46}$ (**31**) and 2-{$Me_2NCH_2CH_2N(Me)CH_2$}C_6H_4HgBr (**32**), were obtained by the reaction of **21** with $HgCl_2$ and $HgBr_2$ in dry THF, respectively. The metathetical reaction of **31**with silver azide afforded air- and moisture-stable organomercury azide, 2-{$Me_2NCH_2CH_2N(Me)CH_2$}$C_6H_4HgN_3$ (**33**) in 87% yield. The transmetallation reaction of **31** with $TeBr_4$ led to isolation of known *o*-formylphenyltellurenyl bromide. All the derivatives were characterized by various spectroscopic techniques such as ^1H, ^{13}C, ^{77}Se, ^{125}Te, ^{199}Hg NMR spectroscopy, elemental analysis, ES-MS and HRMS studies.

Keywords: Pincer Ligand, Organotellurium, Organomercury, Crystal Structure, DFT

1. Introduction

The last decade has witnessed a continuous growth in the development of pincer complexes [1]. The complexes have received a lot of attention mainly due to their involvement in catalysis [2], stabilization of low-valent compounds of main group elements [3] and isolation of reactive intermediates [4]. Generally, the unstable and novel low-valent main group derivatives have been stabilized with the help of tridentate pincer ligands. For example, the isolation of only

three stable organotellurium cations, $[\{2,6\text{-}(Me_2NCH_2)_2C_6H_3\}Te]^+(PF_6)^-$, (**3**) [5], $[\{2,6\text{-}(Me_2NCH_2)_2C_6H_3\}TeO]_2^{2+}(PF_6)_2^-$, (**4**) [6] and $[\{2,6\text{-}\{O(CH_2CH_2)_2NCH_2\}_2C_6H_3\}Te]_2^{2+}(Hg_2Cl_6)^{2-}$, (**6**) [7] has been achieved using substrates (**1**&**5**) where the tellurenium/oxotelluronium cations are stabilized by intramolecular Te···N coordination (Chart 1). Subsequently, a few more crystal structures of analogous organoselenium cations have been reported, e.g. $[\{2,6\text{-}(Me_2NCH_2)_2C_6H_3\}Se]^+(X)^-$, (X = PF_6 [5], Cl, Ph_2SbCl_4 [8], Br [9], $Cl_{0.44}/Br_{0.56}$ [10]). Interestingly, Kersting and DeLion succeeded in isolating the chalcogenols by ortholithiation of **7** followed by Se/Te insertion and hydrolysis with HCl [11]. Further, the oxidation of tellurol, 2-hydrotelluro-N^1, N^3-diisopropylisophthalamide, in presence of base, afforded cyclic product, N,2-diisopropyl-3-oxo-2,3-dihydrobenzo[d][1,2]tellurazole-7-carboxamide (**9**). Similarly, Zade et al. have reported the synthesis of a related product, e.g. 5-*tert*-butyl-2-methyl-7-(methylcarbamoyl)benzisotellurazol-3(2*H*)-one (**10**) [12]. The attempted synthesis of the respective dichalcogenide led to facile cyclisation and isolation of **10**. This benzisotellurazole can be considered as a tellurium analogue of well-known antioxidant 2-phenyl-1,2-benzisoselenazol-3(2H)-one, commonly referred as Ebselen [13]. Recently, Singh and co-workers have reported the tellurenate esters, **14** and **15** and hypervalent diorganyldiacyloxytellurane **16** through the intermediacy of tellurenyl hydroxide **12** and diorganotelluriumdihydroxide **13** [14]**.** The ester groups act as an electrophilic trap for aryltellurenyl hydroxide and are stabilised due to the presence of strong secondary bonding Te···O intramolecular interactions (Chart 1). Selvakumar et al. have focused on OCO and OCN type pincer ligands to investigate the unprecedented sensitivity of secondary bonding interaction (SBI) towards intramolecular steric force present in 2,6-disubstituted arylchalcogen compounds [15]. The study revealed that the isolation of unstable intermediates as their cyclised form,

synthesis of heterocycles and spirocycles by the induction of steric stress at the molecular scale is very productive [15].

In continuation of our studies on intramolecularly coordinated organochalcogens, we now report here the first examples of organotellurium(IV) and organomercury(II) compounds derived from *cis*-pincer *N,N',C*- tridentate 2-{$Me_2NCH_2CH_2N(Me)CH_2$}C_6H_4Br (**20**) ligand. As compared to the *trans*-pincer (N,C,N) ligands, the chemistry of the *cis*-pincer ligands bearing main group derivatives is limited to only organolithium [16] and organotin [17] derivatives. During our investigations on the *cis*-pincer ligand, one example of diorganodiselenide, [2-{$Me_2NCH_2CH_2N(Me)CH_2$}C_6H_4Se]$_2$ has been described by Mugesh *et al.* as glutathione peroxidise mimetics [18]. In addition to this, there have been two more reports on serendipitous formation of *N,N',C*-bound tellurium (IV) derivatives [*N,N',C*-bound $TeCl_3$ (**18**) [19a] and *N,N',C*-bound $TeBr_3$ (**19**) [19b] which were isolated while attempting coordination of $TeCl_4$/$TeBr_4$ with **17**. The *cis*-pincer complexes of **20** with transition metal (Ti [20], Ta [21], W [22], Rh [23], Ir [23], Ni [24], Pd [25], Pt [23], Cu [26], Ag [26], and Au [26]) complexes have been extensively studied.

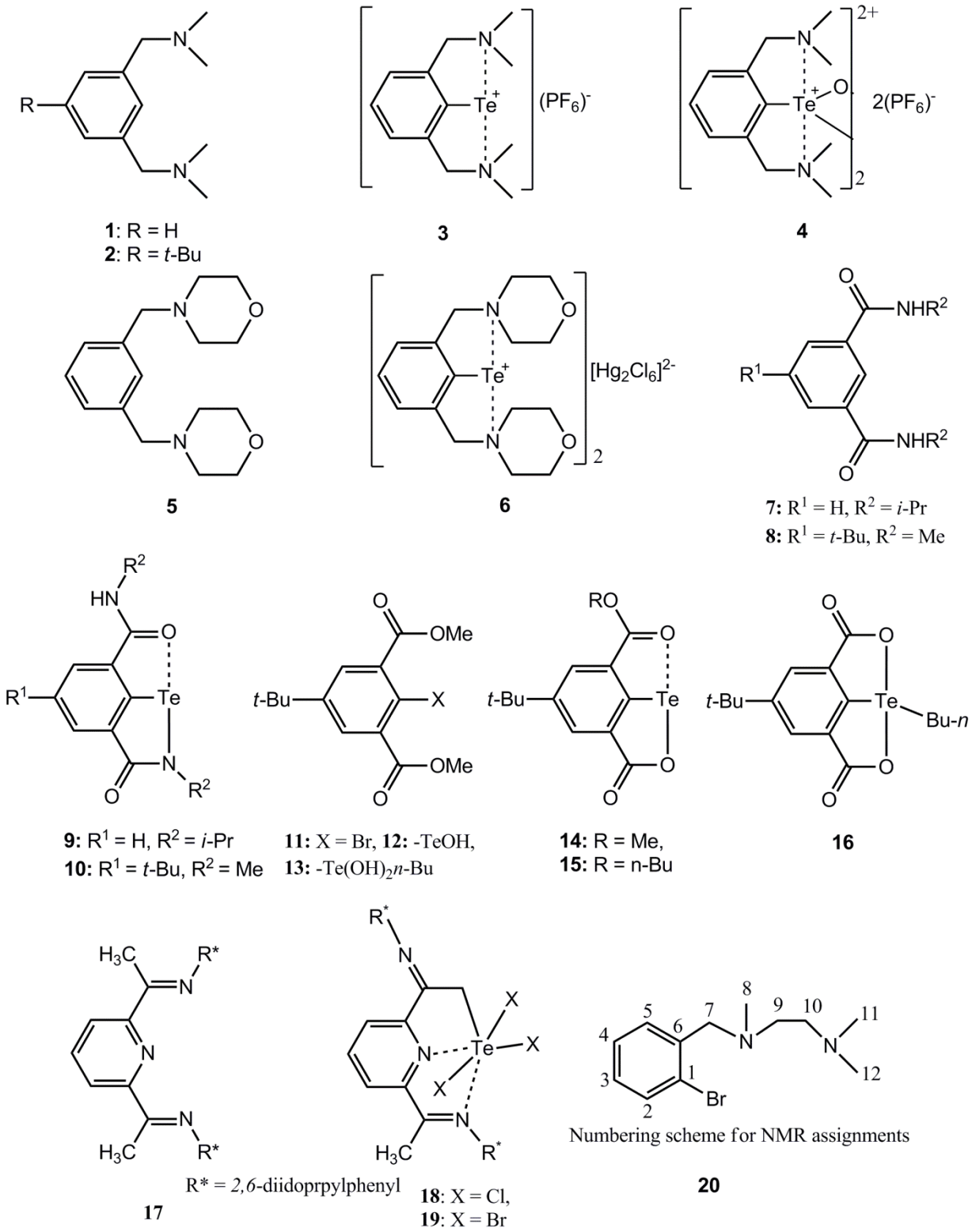

Chart 1. Representatives of organotellurium cationic and neutral species with *trans*- pincer ligands.

2. Experimental

2.1. Caution

The reactions involving mercury compounds and their azide derivative were carried out in a well-ventilated fume hood with proper precautions due to their hazardous nature.

2.2. Materials and methods

Solvents were dried and distilled by standard procedures. Selenium, tellurium, mercury(II) chloride, mercury(II) bromide, bromine, iodine were purchased from Aldrich. Magnesium metal, sodium azide and silver nitrate were purchased from Sisco Research Laboratories, India. 2-{$Me_2NCH_2CH_2N(Me)CH_2$}C_6H_4Br (**20**) [16a], TeI_2 [27], $Se(dtc)_2$ [28] and $Te(dtc)_2$ [28] were prepared according to literature procedures. Chlorine gas was generated by treating $KMnO_4$ with conc. HCl. Silver azide was freshly prepared by reacting of NaN_3 and $AgNO_3$ in water. Melting points were recorded in capillary tubes and are uncorrected. The ^1H, ^{13}C, ^{77}Se and ^{125}Te NMR spectra were recorded on a Varian VXR 400 spectrometer. Chemical shifts cited were referenced to TMS (^1H, ^{13}C) as internal and Me_2Se (^{77}Se) as external standard. The ^{125}Te NMR spectra were recorded on Bruker AMX 400 instruments with dimethyl telluride (Me_2Te) as reference. Electron spray mass spectra (ESI-MS) were performed on a Q-Tof micro (YA-105) mass spectrometer. Mass spectra were obtained with a Platform II single quadrupole mass spectrometer (Micromass, Altrincham, UK) using a CH_3CN mobile phase. Elemental analyses were performed on a Carlo-Erba model 1106 elemental analyzer. IR spectra were recorded as KBr pellets on a Nicolet Impact 400 and Perkin FT-IR spectrometer.

2.3. Synthetic procedures

*2.3.1. Synthesis of [2-{$Me_2NCH_2CH_2N(Me)CH_2$}$C_6H_4E]_2$ (E = Se (**24**); Te (**25**)*

In a 100-mL two-necked flask, magnesium (0.15 g, 6.17 mmol) was taken up in 15 mL of anhydrous THF. To this, compound **20** (1.10 mL, 5.34 mmol) was added drop-wise with constant stirring under reflux conditions. The stirring was continued until the completion of the reaction as indicated by the disappearance of magnesium. Selenium (0.43 g, 5.34 mmol) or tellurium powder (0.68 g, 5.34 mmol) was added to the reaction mixture in portions over a period of 15 min. After 2 h of stirring, the solution was poured into a 50 mL solution of NH_4Cl in water which was kept open for 2 hr for aerial oxidation. The product was extracted with ether (2x50 mL). The ether solution was washed with water and the organic layer was separated, dried over sodium sulfate and evaporated under vacuum to give yellow dense liquid of **24**/**25** respectively.

*Data For **24***; Yield 0.85 g (59%); ^{1}H NMR (400 MHz, $CDCl_3$) δ 2.22 {6 H, s, H-11, 12, N(C*H*$_3$)$_2$}, 2.23 (3 H, s, H-8, NC*H*$_3$), 2.42-2.52 (4 H, m, H-9, 10, N-C*H*$_2$-C*H*$_2$-N), 3.51 (2 H, s, H-7, C_6H_4–C*H*$_2$–N), 7.29-7.36 (4 H, m, H-2–5, C_6*H*$_4$); ^{13}C NMR (100.6 MHz, $CDCl_3$) δ 42.47 (s, C-8), 45.73 (s, C-11), 45.80 (s, C-12), 55.06 (s, C-9), 57.32 (s, C-10), 62.9 (s, C-7), 126.94 (s, C-3), 128.11 (s, C-4), 128.15 (s, C-5), 128.20 (s, C-2), 129.07 (s, C-1), 138.80 (s, C-6); ^{77}Se NMR (76.3 MHz, $CDCl_3$) δ 425.6. HRMS 543.1508 $[M]^+$.

For **25**; Yield 1.56 g (46%); ^{1}H NMR (400 MHz, $CDCl_3$) δ 2.18{6 H, s, H-11, 12, N(C*H*$_3$)$_2$}, 2.23 (3 H, s, H-8, NC*H*$_3$), 2.50-2.57 (4 H, m, H-9, 10, N-C*H*$_2$-C*H*$_2$-N), 3.61 (2 H, s, H-7, C_6H_4–C*H*$_2$–N), 6.97-6.98 (2 H, m, H-3, 4, C_6*H*$_4$), 7.08 (1 H, m, H-5, C_6*H*$_4$), 7.95 (1 H, d, H-2, C_6*H*$_4$); ^{13}C NMR (100.6 MHz, $CDCl_3$) δ 40.73 (s, C-8), 45.59 (s, C-11), 45.74 (s, C-12), 54.12 (s, C-9), 57.03 (s, C-10), 65.37 (s, C-7), 112.82 (s, C-1), 126.30 (s, C-3), 128.14 (s, C-4, 5), 139.00 (s, C-2), 140.89 (s, C-6); ^{125}Te NMR (126.3 MHz, $CDCl_3$) δ 347.3.

*2.3.2. Synthesis of [2-{$Me_2NCH_2CH_2N(Me)CH_2$}C_6H_4]$_2$Se (**26**)*

Method (a)

To a freshly prepared Grignard solution of **20** (0.5 mL, 2.6 mmol) in THF, was added a solution of $Se(dtc)_2$ (0.375 g, 1.00 mmol) in the same solvent at -72 ^oC. Then, the mixture was stirred for 14 h to complete the reaction. The solution was poured into 50 mL water. The product was extracted with ether (4 x50 mL). The ether solution was washed with water and the organic layer was separated, dried over sodium sulfate and evaporated under vacuum to give an orange coloured dense liquid. The dense liquid was further purified by flash column chromatography by using 30% of ethyl acetate and petroleum-ether (40-60) which afforded orange coloured dense liquid of **26** (0.25g, 54% yield).

Method (b)

To a solution of **20** (0.5mL, 2.6 mmol) in dry hexane (10 mL), was added a 1.6 M solution of n-butyllithium in hexane (3.4 mL, 5.5 mmol) via syringe under N_2 at room temperature. This was stirred for 2h at room temperature and allowed to settle. The solvent was removed by syringe and the white lithiated precipitate was dissolved in dry THF (20 mL). This was added to a solution of $Se(dtc)_2$ (0.488 g, 1.3 mmol) at -72 ^oC. Then the mixture was stirred for 14 h to complete the reaction. Further workup of the reaction mixture and purification as described in method (a) afforded a dense liquid of **26** (0.31 g, 67% yield). ^1H NMR (400 MHz, $CDCl_3$) δ 2.24 (3 H, s, H-8, NCH_3), 2.33{6 H, s, H-11, 12, $N(CH_3)_2$}, 2.60 (4 H, m, H-9, 10, N-CH_2-CH_2-N), 3.53 (2 H, s, H-7, C_6H_4–CH_2–N), 7.30-7.88 (4 H, m, H-2–5, C_6H_4); ^{13}C NMR(100.6 MHz,$CDCl_3$) δ 41.47 **(**s, C-8), 44.68 (s, C-11, 12), 53.81 (s, C-9), 56.12 (s, C-11, 10), 61.89 (s, C-7), 126.07 (s, C-3), 127.25 (s, C-4, 5), 127.73 (s, C-2), 128.17 (s, C-1), 137.72 (s, C-6);^{77}Se NMR (76.3 MHz, $CDCl_3$) δ 422.2 ppm**.**

*2.3.3. Synthesis of [2-{$Me_2NCH_2CH_2N(Me)CH_2$}C_6H_4]Te{$S_2CN(CH_2CH_3)_2$} (**27**)*

Compound **27** was also prepared following the method (a) by using $Te(dtc)_2$ (1.10 g, 2.6 mmol) in place of $Se(dtc)_2$. The isolated compound was a dense liquid (0.28g, 60% yield). ^{1}H NMR (400 MHz, $CDCl_3$) δ 1.27 {3 H, t, $SCN(CH_2CH_3)_2$}, 1.34 {3 H, t, $SCN(CH_2CH_3)_2$}, 2.30 {6 H, s, H-11, 12, $N(CH_3)_2$}, 2.53 (3 H, s, H-8, NCH_3), 2.68 (4 H, m, H-9, 10, N-CH_2-CH_2-N), 3.50 (2 H, s, H-7, C_6H_4–CH_2–N), 3.95 {2 H, q, $SCN(CH_2CH_3)_2$}, 4.04 {2 H, q, $SCN(CH_2CH_3)_2$}7.13 (2 H, m, H-3, 4, C_6H_4), 7.31 (1 H, m, H-5, C_6H_4), 7.77 (1 H, d, H-2, C_6H_4); ^{125}Te NMR (126.3 MHz, $CDCl_3$) δ 1083.3 ppm; ES-MS *m/z* (relative intensity, nature of peak) 321 (30, $[2\text{-}\{Me_2NCH_2CH_2N(Me)CH_2\}C_6H_4Te]^+$); 529 (100, $[\{2\text{-}\{Me_2NCH_2CH_2N(Me)CH_2\}C_6H_4\}_2Te+OH]^+$.

*2.3.4. Synthesis of $[2\text{-}\{(Me_2NH)CH_2CH_2N(Me)CH_2\}C_6H_4TeI]^+(I)^-$ (**28a**)*

To a freshly prepared Grignard solution of **20** (1 mL, 5.34 mmol) in THF, was added TeI_2 (2.01 g, 5.34 mmol). Then the mixture was stirred for 12 h to complete the reaction. The resulting solution was poured into 50 mL water. The product was extracted with chloroform (4x50 mL). The chloroform solution was washed with water and the organic layer was separated, dried over sodium sulfate, and filtered to give an orange coloured solution. The solution was concentrated to 5 mL under vacuum. The solution was cooled in freeze at 0 ^{o}C for 24 h to give needle shaped crystals of **28a** (0.45 g, 15% yield). The crystals were separated by decantation and washed with hexane. M.p. 197-198 °C. ^{1}H NMR (DMSO-d_6) δ 2.74 (3 H, s, H-8, NCH_3), 2.88 {6 H, s, H-11, 12, $N(CH_3)_2$}, 3.25 (2 H, m, H-10, N-CH_2-CH_2-N), 3.41 (2 H, m, H-9, N-CH_2-CH_2-N)), 4.15 (2 H, s, H-7, C_6H_4–CH_2–N), 7.28 (3 H, m, H-3–5, C_6H_4), 7.84 (1 H, d, H–2, C_6H_4); ^{13}C NMR (100.6 MHz, DMSO-d_6) δ 43.10 (s, C-11, 12), 43.67 (s, C-8), 51.67 (s, C-10), 52.87 (s, C-9), 64.56 (s, C-7), 116.82 (s, C-1), 127.34 (s, C-3), 127.69 (s, C-4), 129.32 (s, C-5),

137.44 (s, C-2), 139.23 (s, C-6); ES-MS *m/z* (relative intensity, nature of peak) 449 (22, $[M]^+$); 321 (90, $[M-I]^+$); ^{125}Te NMR (126.3 MHz, DMSO-d_6) δ 1249.

*2.3.5. Synthesis of [2-{(Me$_2$NH)CH$_2$CH$_2$N(Me)CH$_2$}C$_6$H$_4$TeCl$_3$]$^+$(Cl)$^-$ (**29a**)*

To a 25 mL dry THF solution of **25** (1.35 g, 2.11 mmol), was passed, freshly prepared dry Cl_2 gas for 30 min. at 60 °C to afford a white ppt. of **29a**. The precipitate obtained was recrystallized from DMSO solvent to give colourless crystal of **29a** (0.73 g, 74% yield). M.p. 186-188 °C. ^{1}H NMR (400 MHz, CD_3OD) δ 2.84 (3 H, s, H-8, NC*H*$_3$), 2.98 {6 H, s, H-11, 12, N(C*H*$_3$)$_2$}, 3.72 (4 H, m, H-9, 10, N-C*H*$_2$-C*H*$_2$-N), 4.48 (2 H, s, H-7, C$_6$H$_4$–C*H*$_2$–N), 7.52 (3 H, m, H-3–5, C$_6$*H*$_4$), 7.65 (1 H, d, H–2, C$_6$*H*$_4$); ^{13}C NMR (100.6 MHz, DMSO-d_6) δ41.96 (s, C-11), 42.70 (s, C-12), 43.42 (s, C-8), 50.82 (s, C-10), 51.05 (s, C-9), 61.79 (s, C-7), 128.13 (s, C-1), 130.29 (s, C-3), 131.03 (s, C-4), 131.95 (s, C-5), 139.40 (s, C-2), 145.24 (s, C-6); ^{125}Te NMR (126.3 MHz, DMSO-d_6) δ 1363.1.

*2.3.6. Synthesis of [2-{(Me$_2$NH)CH$_2$CH$_2$N(Me)CH$_2$}C$_6$H$_4$TeBr$_3$]$^+$(Br)$^-$(**30a**)*

To a 25 mL dry THF solution of **25** (1.70 g, 2.67 mmol), was added drop-wise Br_2 (0.43 g, 2.67 mmol) solution in the same solvent for 15 min. at 60 °C to afford a yellow precipitate of **30a** (1.14 g, 67% yield). The precipitate obtained was recrystallized from DMSO solvent to give yellow crystals of **30a.** M.p. 171 °C. ES-MS *m/z* (relative intensity, nature of peak) 479 (40, $[M-Br]^+$); 417 (100, $[M-Br+OH]^+$); ^{125}Te NMR (126.3 MHz, DMSO-d_6) δ 1438.7; Anal. Calcd. for $C_{12}H_{19}N_2Te\ Br_3$.HBr: C, 22.54; N, 4.38; H, 3.15. Found C, 23.10; N, 5.42, H, 3.05.

*2.3.7.Synthesis of [2-{Me$_2$NCH$_2$CH$_2$N(Me)CH$_2$}C$_6$H$_4$]HgCl$_{0.54}$/Br$_{0.46}$(**31**)*

To a freshly prepared Grignard solution of **20** (1.1 mL, 5.34 mmol) in THF, was added a solution (15 mL) of $HgCl_2$ (0.35 g, 2.06 mmol) in the same solvent and the reaction mixture was stirred further for 12 h. The reaction mixture was concentrated to 5 mL under vacuum. The

residue was treated with water and the resulting aqueous solution was extracted with chloroform. The organic layer was separated and dried over sodium sulphate. The resulting solution was filtered, concentrated to 5 mL and cooled to 0 ^{o}C to give colourless rhomboidal crystals of **31** (0.68g, 30% yield). M.p. 162 °C. FT-IR (KBr) 3041, 2982, 2963, 2949, 2841, 2825, 2791, 1448, 1434 1297, 1020, 962, 929, 798, 773, 744 cm^{-1}; ^{1}H NMR (400 MHz, $CDCl_3$) δ 2.03 ({6 H, s, H-11, 12, N(CH_3)$_2$}, 2.48 (4 H, br, H-9, 10, N-CH_2-CH_2-N), 2.55 (3 H, s, H-8, NCH_3), 3.55, (2 H, s, H-7, C_6H_4–CH_2–N), 7.14-7.23 (3 H, m, H-3–5, C_6H_4), 7.43 (1 H, d, H–2, C_6H_4); ^{13}C NMR (100.6 MHz, $CDCl_3$) δ 43.43 (s, C-8), 45.73 (s, C-11, 12), 53.42 (s, C-9), 57.66 (s, C-10), 63.82 (s, C-7). 127.14 (s, C-3), 127.61 (s, C-4, 5), 128.85 (s, C-1), 137.57 (s, C-2), 143.82 (s, C-6); ^{199}Hg NMR (400 MHz, $CDCl_3$) -879.6, -996.1; HRMS 429.1008 (100, [M-Br]$^{+}$), 473.0479 (60, [M-Cl]$^{+}$); Anal. Calcd. for $C_{12}H_{19}N_3HgCl$: C, 33.73; N, 6.56; H, 4.48. Found C, 32.16; N, 6.19; H, 4.51.

*2.3.8. Synthesis of [2-{$Me_2NCH_2CH_2N(Me)CH_2$}C_6H_4]HgBr(**32**)*

Compound **32** was prepared from $HgBr_2$ (0.11 g, 5.34 mmol) and a freshly prepared Grignard solution of **20** (1.1 mL, 5.34 mmol) in a similar way described for **31**.It afforded colourless rectangular shaped crystals of **32** (0.96 g, 38% yield). M.p. 151-152 °C. ^{1}H NMR (400 MHz, $CDCl_3$) δ 2.02 {6 H, s, H-11, 12, N(CH_3)$_2$}, 2.39 (4 H, br, H-9, 10, N-CH_2-CH_2-N), 2.54 (3 H, s, H-8, NCH_3), 3.55, (2 H, s, H-7, C_6H_4–CH_2–N), 7.16-7.24 (3 H, m, H-3–5, C_6H_4), 7.43 (1 H, d, H–2, C_6H_4); Anal. Calcd. for $C_{12}H_{19}N_3HgBr$: C, 30.55; N, 5.94; H, 4.06. Found C, 30.37; N, 6.08; H, 3.88.

*2.3.9. Synthesis of [2-{$Me_2NCH_2CH_2N(Me)CH_2$}C_6H_4]HgN_3 (**33**)*

To a solution of **31** (0.24 g, 0.50 mmol) in 10 mL chloroform, was added 5 mL solution of silver azide (0.60 g, 4.00 mmol) in methanol. The reaction mixture was stirred at room

temperature for 12 h and the precipitate filtered off. The filtrate was concentrated by removing the solvent under vacuum to afford a crystalline solid of **33** (0.19 g, 87% yield). ^{1}H NMR (400 MHz, $CDCl_3$) δ 2.06 {6 H, s, H-11, 12, N(CH_3)$_2$}, 2.40 (4 H, br, H-9, 10, N-CH_2-CH_2-N), 2.57 (3 H, s, H-8, NCH_3) 3.55 (2 H, s, H-7, C_6H_4–CH_2–N), 7.16-7.20 (3 H, m, H-3–5, C_6H_4), 7.40 (1 H, d, H–2, C_6H_4); ^{13}C NMR (100.6 MHz, $CDCl_3$) δ 43.74 (s, C-8), 45.67 (s, C-11, 12), 53.55 (s, C-9), 58.06 (s, C-10), 64.06 (s, C-7), 127.18 (s, C-3), 127.83 (s, C-4), 128.94 (s, C-5), 137.72 (s, C-1), 143.62 (s, C-6); FT-IR (KBr) 2827, 2055 (HgN_3), 1450, 1297, 1030, 964, 800, 745 cm^{-1}; HRMS *m/z* (Calculated 458.1241), 458.1235 $[M+Na]^+$; Anal. Calcd. for $C_{12}H_{19}HgN_3$: C, 33.22; N, 16.14; H, 4.41. Found C, 33.41; N, 12.84; H, 4.05.

2.3.10. X-Ray Crystallographic Study

The single crystal X-ray diffraction measurements were performed on an Oxford Diffraction Gemini diffractometer and Rigaku Saturn 724 diffractometer. The data were corrected for Lorentz, polarization, and absorption effects. The structures were determined by routine heavy-atom methods using SHELXS 97 [29] and Fourier methods and refined by full-matrix least squares with the non-hydrogen atoms anisotropic and hydrogen with fixed isotropic thermal parameters of 0.07 Å using the SHELXL 97 [29] program. The hydrogen atoms were partially located from difference electron density maps, and the rest were fixed at predetermined positions. Scattering factors were from common sources [30]. The details of crystal data and structure refinement for **28a-30a** and **31-33** are given in Table 1. CCDC-1814430 (**28a**), CCDC-1814428 (**29a**), CCDC-

1814425 (**30a**), CCDC-1814429 (**31**), CCDC-1814431 (**32**) and CCDC-1814427 (**33**) contain the supplementary crystallographic data for this paper.

Table 1 Crystallographic Data and Refinement Details for **28a, 29a, 30a, 31**, **32** and **33**.

Compound	**28a**	**29a**	**30A**	**31**	**32**	**33**
Empirical formula	$C_{12}H_{20}I_2N_2Te$	$C_{12}H_{20}Cl_4N_2Te$	$C_{12}H_{20}Br_4N_2Te$	$C_{12}H_{19}Br0.45Cl0.55HgN_2$	$C_{12}H_{19}BrHgN_2$	$C_{12}H_{19}HgN_5$
Formula weight	573.70	461.70	639.54	447.34	471.79	433.91
Crystal system	Monoclinic	Monoclinic	Monoclinic	Monoclinic	Monoclinic	Triclinic
Space group	$P2_1/c$	$P2_1/c$	$P2_1/c$	$P2_1/n$	$P2_1/n$	P-1
a (Å)	11.0462(11)	16.8680(11)	17.1102(9)	10.1848(5)	10.2034(2)	9.2245(7)
b (Å)	15.3693(16)	7.7538(5)	7.9362(4)	9.5247(5)	9.5432(2)	9.4152(8)
c (Å)	10.1845(11)	13.5941(10)	14.0464(7)	14.3746(7)	14.4962(4)	9.4569(7)
α (°)	90	90	90	90	90	89.764(7)
β (°)	99.366(10)	100.865(7)	102.493(5)	98.762(5)	98.632(2)	69.016(7)
γ (°)	90	90	90	90	90	79.020(7)°
V ($Å^3$)	1706.0(3)	1746.1(2)	1862.20(16)	1378.15(12)	1395.55(6)	750.99(11)
Z	4	4	4	4	4	2
D(calcd) (Mg/m^3)	2.234	1.756	2.281	2.156	2.246	1.919
T (K)	123(2)	123(2)	173(2)	123(2)	123(2)	296(2)
Range of θ(deg)	4.06 to 67.70	6.30 to 75.74	2.96 to 28.28	3.14 to 35.02	4.97 to 75.69	4.80 to 75.57
Abs coeff (mm^{-1})	42.049	18.990	10.171	12.556	22.941	18.311
Obsdreflens[I >σ]	3351	3578	4609	5629	2809	3012
Final R_1 [I > 2σ(I)]	0.0844	0.0553	0.0543	0.0635	0.0431	0.0415
wR_2 indices [I >σ]	0.2234	0.1306	0.0935	0.0756	0.0928	0.0782
Data/Restr./Param.	3351/6/157	3578/0/175	4609/1/178	5629/8/159	2809/0/148	3012/0/166
Goodness of fit F^2	1.055	1.102	1.060	0.985	1.064	1.030

2.3.11. Computational Details

All density functional theory (DFT) calculations were performed with the aid of Gaussian 09 suite of quantum chemical programs [31]. The geometries of the compounds **28-33** were optimized with B3LYP functional [32] by employing 6-311+G(d) basis set for H,C,N and Lanl2dz basis set for Cl, Br, Te and Hg. The optimized geometries were confirmed as minima by the frequency calculations on the optimized geometries. Natural Bond Orbital (NBO) analysis [33] and Atoms in Molecules (AIM) [34] calculations were performed using the DFT -optimized structures at the same level of theory. AIM calculations were performed with the help of Multiwfn software [35] and the computed structures of the compounds were visualized with ChemCraft program [36].

3. Results and discussion

3.1. Synthesis

The precursor, 2-{$Me_2NCH_2CH_2N(Me)CH_2$}C_6H_4Br (**20**) was prepared by following the reported procedure [16]. Lithiation of **20** was carried out with an excess of *n*-BuLi (1:2 ratio) at -78 °C followed by the addition of Se that afforded a viscous liquid of N^1-(2-(butylselanyl)benzyl)-N^1,N^2,N^2-trimethylethane-1,2-diamine (**23**), instead of the expected diaryldiselenide, [2-{$Me_2NCH_2CH_2N(Me)CH_2$}$C_6H_4Se]_2$ (**24**). The ^{1}H NMR spectrum of **23** exhibited some more peaks along with the peaks for the butyl group. To purify **23**, it was derivatized by complexing with $HgCl_2$ that afforded [2-{$Me_2NCH_2CH_2N(Me)CH_2$}C_6H_4SeBu-*n*]$HgCl_2$ (For experimental details, molecular structure and spectra, see Supporting Information pages S3-S10) **[37]**. To avoid the formation of the undesired product **23**, alternatively, Grignard route was used. A freshly prepared Grignard reagent, 2-{$Me_2NCH_2CH_2N(Me)CH_2$}C_6H_4MgBr (**21**) in THF, was treated with Se/Te followed by oxidative workup to provide **24**/ [2-{$Me_2NCH_2CH_2N(Me)CH_2$}$C_6H_4Te]_2$ (**25**) as major products. Compound **24** was isolated in better yield (59%) compared with the reported lithiation route (42%) [18]. Compounds [2-{$Me_2NCH_2CH_2N(Me)CH_2$}$C_6H_4]_2Se$ (**26**) and [2-{$Me_2NCH_2CH_2N(Me)CH_2$}C_6H_4]Te($S_2CN(CH_2CH_3)_2$ (**27**) were synthesized by the reaction of **21**/**22** with $Se(dtc)_2$ in 2:1 and $Te(dtc)_2$ in 1:1 ratio at room temperature (dtc = diethyldithiacarbamate). Similarly, the reaction of **21** with TeI_2 leads to the formation of an orange solid of [2-{(Me_2NH)$CH_2CH_2N(Me)CH_2$}C_6H_4Tel]$^+$(I)$^-$ (**28a**). Compounds, **23-27** were isolated as viscous liquids and all attempts to solidify these were unsuccessful. In order to study the Te···N intramolecular interactions in the solid state, halogen derivatives were prepared (*vide infra*). The reactions of **25** with halogenating agents; chlorine gas or a THF solution of bromine,

in 1:1 or 1:3 molar ratio led to isolation of corresponding organotellurium halides as viscous liquids and in no case the desired solids; LTeCl/LTeBr/$LTeCl_3$(**29**)/$LTeBr_3$(**30**) (L= 2-{$Me_2NCH_2CH_2N(Me)CH_2$}C_6H_4), could be isolated. However, when an excess of the halogenating agent was added to **25** in THF, it led to immediate precipitation of white and yellow powdered solids of [2-{$(Me_2NH)CH_2CH_2N(Me)CH_2$}$C_6H_4TeCl_3$]$^+(Cl)^-$ (**29a**)/ [2-{$(Me_2NH)CH_2CH_2N(Me)CH_2$}$C_6H_4TeBr_3$]$^+(Br)^-$ (**30a**), respectively (Scheme 1). Compounds **28a**, **29a** and **30a** have low solubility in common organic solvents, however, these could be crystallized from DMSO. The initial characterization by IR spectroscopy indicated the presence of NH stretching frequency at 3440 cm^{-1} for **30a** indicating protonation of one of the amine nitrogen atoms. This was further confirmed by single crystal X-ray studies (*vide infra*). The solubility behaviors of **28a** and **29a** with **30a** indicated that these were also protonated (*vide infra*). Attempted deprotonation of these to obtain the corresponding neutral organotellurium halides (**28-30**) by treatment with saturated aqueous $NaHCO_3$ solution or aqueous NaOH (10%) were unsuccessful.

Alternatively, to circumvent the facile protonation, it was planned to use organomercury derivatives as precursors for the isolation of **28-30** by transmetallation reaction with TeI_2, $TeCl_4$, and $TeBr_4$ respectively. For this, organomercurial compound 2-{$Me_2NCH_2CH_2N(Me)CH_2$}C_6H_4HgCl (**31**), was prepared by the treatment of LMgBr with $HgCl_2$. Complex **31** was co-crystallized with complex 2-{$Me_2NCH_2CH_2N(Me)CH_2$}C_6H_4HgBr (**32**). The co-crystallisation was confirmed by elemental analysis, HRMS, ^{199}Hg NMR and X-ray structure determination (*vide infra*). Recently, similar co-crystallisation of the organomercury chloro- and bromo-derivatives has been observed in the case of {2,6-$(Me_2NCH_2)_2C_6H_3$}$HgCl_{0.70}/Br_{0.30}$ [38]. Pure complex **32** could be prepared by using $HgBr_2$ in

place of $HgCl_2$. Both the complexes **31** and **32** are highly soluble in common organic solvents and are crystalline in nature. The reaction of **32** with $TeBr_4$ led to the isolation of *o*-formylphenyltellurenyl bromide [39]. This probably forms by the protonation of amine nitrogen atom followed by hydrolysis (Scheme S2, see Supporting Information page S4) [40]. The azide derivative **33** was synthesizedby the metathesis of **31** with silver azide.

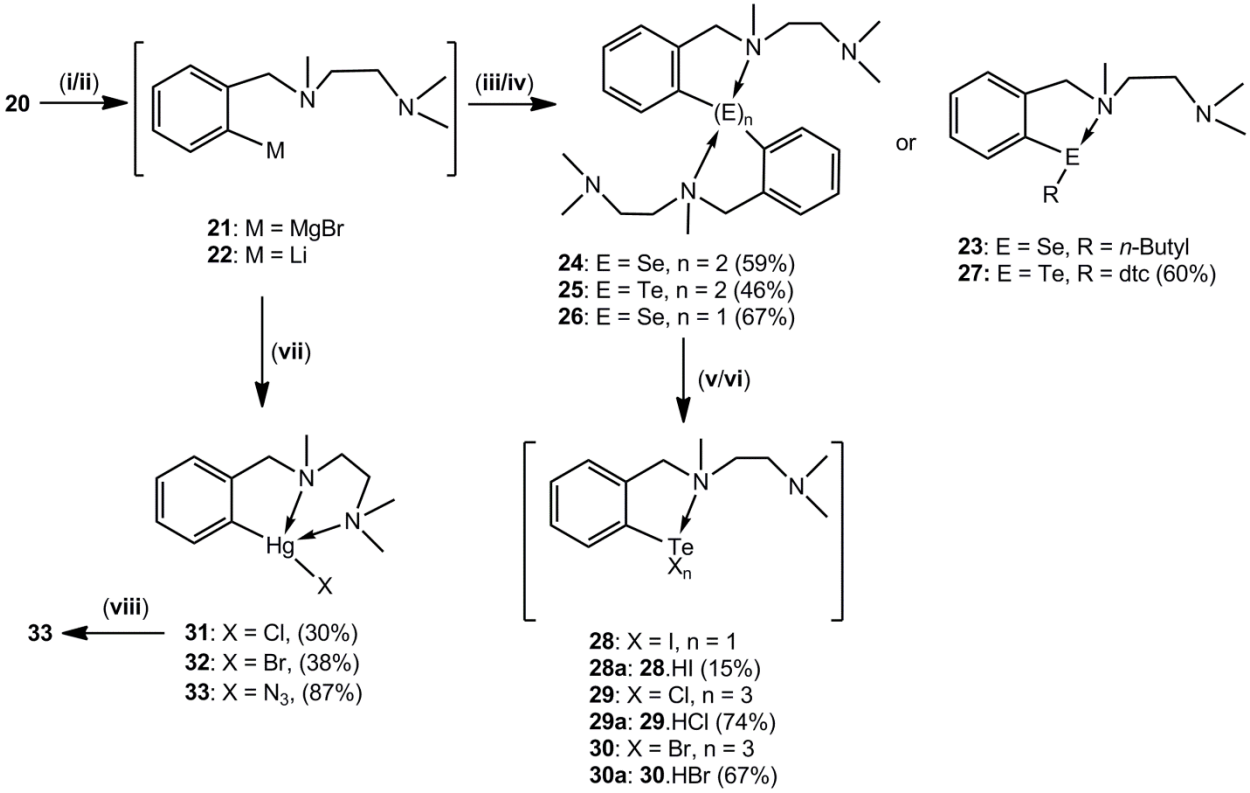

Scheme 1. Synthesis of organochalcogen (**23-30**, **28a-30a**) and organomercury (**31-33**) derivatives. Conditions: (i) Mg, I_2, THF; (ii) *n*-BuLi, Et_2O, 3h, -78 °C; (iii) Se/Te, 6 h, room temperature (rt), [O_2]; (iv) $Se(dtc)_2$ (2:1)/[$Te(dtc)_2$ (1:1), Et_2O, 12h, rt; (v) TeI_2, THF, 2h, 60 °C; (vi) Cl_2/Br_2, THF, 2h, 60 °C (vii) $HgCl_2/HgBr_2$, 6h, rt (viii) AgN_3, $CHCl_3$, 12h, rt.

3.2. Spectroscopic Studies

3.2.1. NMR Spectroscopic Studies

The complexes were characterized by ^{1}H, ^{13}C, ^{77}Se, ^{125}Te, ^{199}Hg NMR spectroscopy. The ^{1}H NMR spectrum of the organoselenium and tellurium complexes showed sharp singlet and triplet for C(aryl)CH_2N and NCH_2CH_2N protons. Interestingly, the ^{1}H NMR spectra of **31, 32** and **33** exhibit broad peaks for all the three sets of CH_2 protons and the NMe_2 group appeared as singlet. The broad peaks may be due to plausible dynamic coordination of $–NMe_2$ in the solution state. A possible fluxional process could be an association-dissociation process involving the $Hg–NMe_2$ bond, a phenomenon which has been observed in other NN'C-bound metal complexes [20, 23b]. The ^{77}Se NMR spectra of **24** and **26** exhibited peaks at 425 and 422 ppm, respectively and the chemical shift values are in the range reported for diaryldiselenide and diarylselenide [41]. The ^{125}Te NMR chemical shifts for **25**, **27**, **28a**, **29a** and **30a** appear at 347, 1083, 1249, 1363 and 1439 ppm, respectively. The signal observed at δ = 1083 ppm in the ^{125}Te NMR spectrum of **27** is shifted upfield relative to that observed for **28a** (δ = 1249 ppm), **29a** (δ = 1363 ppm) and **30a** (δ = 1439 ppm). This trend can be ascribed to the presence of electron withdrawing iodo, chloro and bromo groups at the Te center in **28a**, **29a** and **30a**, respectively. The ^{199}Hg NMR signals for **31** and **32** are shifted upfield relative to Ph_2Hg (-745 ppm) **[42]**. The shifts may be attributed to +I effect of the amino groups. The ^{199}Hg NMR spectrum of **31** showed two peaks at -966 and -879 ppm for complexes **31** and **32**, respectively confirming the co-crystallisation of **31** with **32**.

3.2.2.Mass Spectrometric Studies

ES-MS of **27** showed three intense peaks at m/z 193, 321 and 529, which were assigned to $[2\text{-}\{(Me_2NH)CH_2CH_2N(Me)CH_2\}C_6H_5]^+$, $[2\text{-}\{Me_2NCH_2CH_2N(Me)CH_2\}C_6H_4Te]^+$, and $[\{2\text{-}\{Me_2NCH_2CH_2N(Me)CH_2\}C_6H_4\}_2Te{+}OH]^+$ respectively. For complex **28a,** sets of peaks for molecular ions $[M]^+$ and $[M\text{-}I]^+$ were observed at *m/z* 449 and 321 respectively. Similarly, the

ES-MS of **30a** showed five sets of peaks for [2-{$Me_2NCH_2CH_2N(Me)CH_2$}$C_6H_4TeBrOH$]$^+$, at *m/z* 416; [2-{$Me_2NCH_2CH_2N(Me)CH_2$}C_6H_4Te]$^+$, at *m/z* 321; [2-{$Me_2NCH_2CH_2N(Me)CH_2$}$C_6H_4TeBr_2$]$^+$, at *m/z* 478; [2-{$Me_2NCH_2CH_2N(Me)CH_2$}$C_6H_4TeBrNa$]$^+$, at *m/z* 423; and [2-{$Me_2NCH_2CH_2N(Me)CH_2$}C_6H_4TeO]$^+$, at *m/z* 337. The HRMS of **31** and **32** exhibited molecular ion peaks at *m/z* 429.1008 and 473.0479, respectively. The peak observed at *m/z* 458.1235 corresponds to complex **33** [M+Na]$^+$ (see Supporting Information, for ES-MS and HRMS spectra). It is worth noting that similar to cations of **3** and **6**, the cation of **28a** is stable and prominently observed in the mass spectrum.

3.3. Crystal structures

*3.3.1. Molecular Structure of **28a***

The molecular geometry around the tellurium(II) atom is distorted T-shaped (Fig. 1). The distance between Te and N1 is 2.426(15) Å and is close to the calculated value of 2.570 Å (Table 2). The Te···N1 distance is much less than the sum of the van der Waals radii, Σ r_{vdw} (Te,N), 3.61 Å [43]. The tellurium atom in **28a** is strongly coordinated by N1 atom whereas N2 atom is protonated. The Te···N1 distances are longer than those observed for [2,6-{$O(CH_2CH_2)_2NCH_2$}$_2C_6H_3Te$]$^+$ (2.372 Å) [6] and shorter than that observed for [2,6-{Me_2NCH_2}$_2C_6H_3TeO$]$_2^{2+}$ (2.475 Å)[7]. The lattice of **28a** molecule exhibits intermolecular C–H···I and N–H···I H-bonding interactions, which give rise to a 2-D supramolecular motif that extends along the crystallographic *a*-axis. (Fig. S44, see Supporting Information page S42).

*3.3.2.Molecular Structures of **29a** and **30a***

The primary geometry around the Te(IV) atoms in these organotellurium trihalides is trigonal bipyramidal with a stereochemically active lone pair (Fig. 2 and 3). Two halogen atoms occupy the axial positions with an X–Te–X (X = Cl and Br) bond angle of 173.21(5)° and 173.97(2)° in **29a** and **30a**, respectively. Interatomic Te···N(1) distances (*d*(Te···N1) 2.437(4) Å in **29a** and 2.463(4) Å in **30a**) are short enough to imply the presence of attractive intramolecular Te···N secondary bonding interactions but larger than that found in **17** [*d*(Te···N1) 2.321(3) Å] [19a] and **19** [*d*(Te···N1) 2.359(3) Å] [19b]. There are no Te···N2 close intermolecular contacts in molecules **29a** & **30a**, though in the case of **18** [*d*(Te···N2) 2.732(3)Å] [19a] and **19** [*d*(Te···N2) 2.793(3)Å] [19b] such interactions are reported. The N1···Te–X2 angles [X = Cl; 169.1(1)° and X = Br; 170.2(1)] are also greater than the [(N1···Te–Cl2)160.9(8)°] [19a] and [(N1···Te–Br2)164.1(8)°] angles [19a]. Complexes **29a** and **30a** show C–H···halogen and N–H···halogen H-bonding interactions which possess the required linearity (~160.86°) and donor-acceptor distance {interatomic d(H···halogen, ~2.7190Å)}. These intermolecular interactions lead to supramolecular assembly into two-dimensional motifs (see Supporting Information page S43-S44).

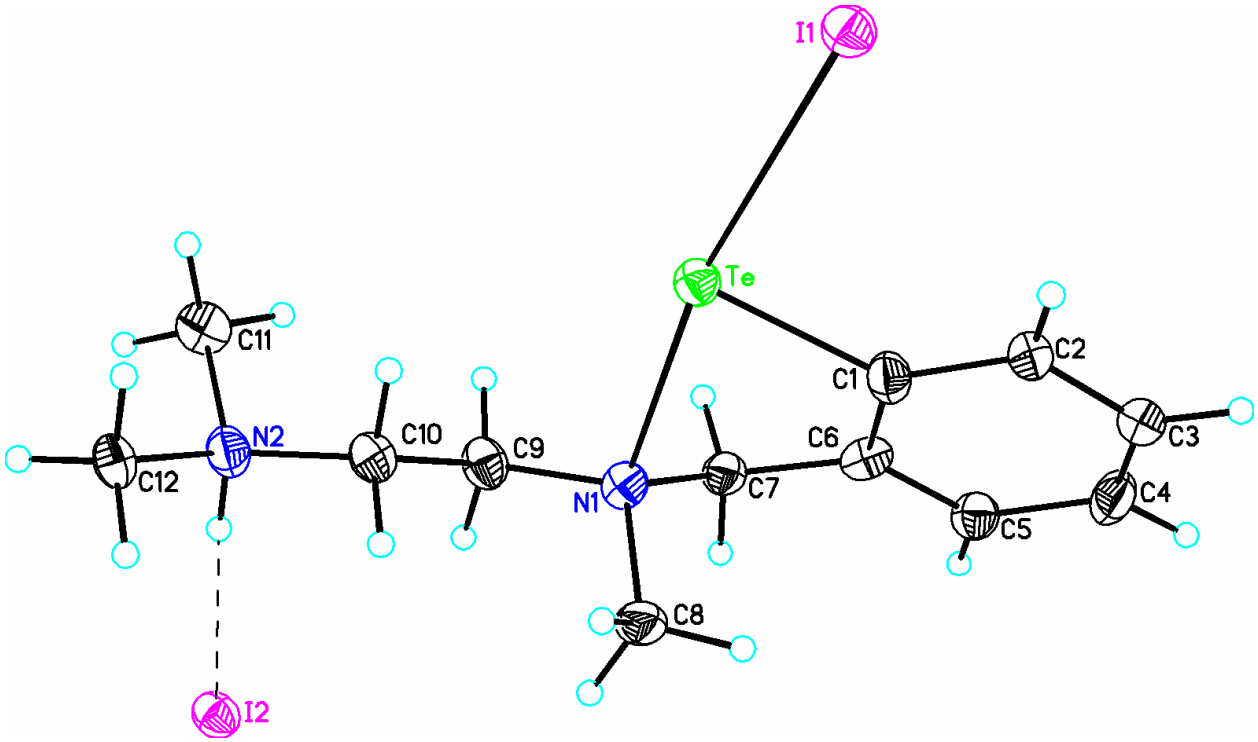

Fig. 1 Molecular structure of **28a** showing 50% probability displacement ellipsoids and the atom numbering scheme. Selected bond distances (Å) and angles (°) are shown in Table 2.

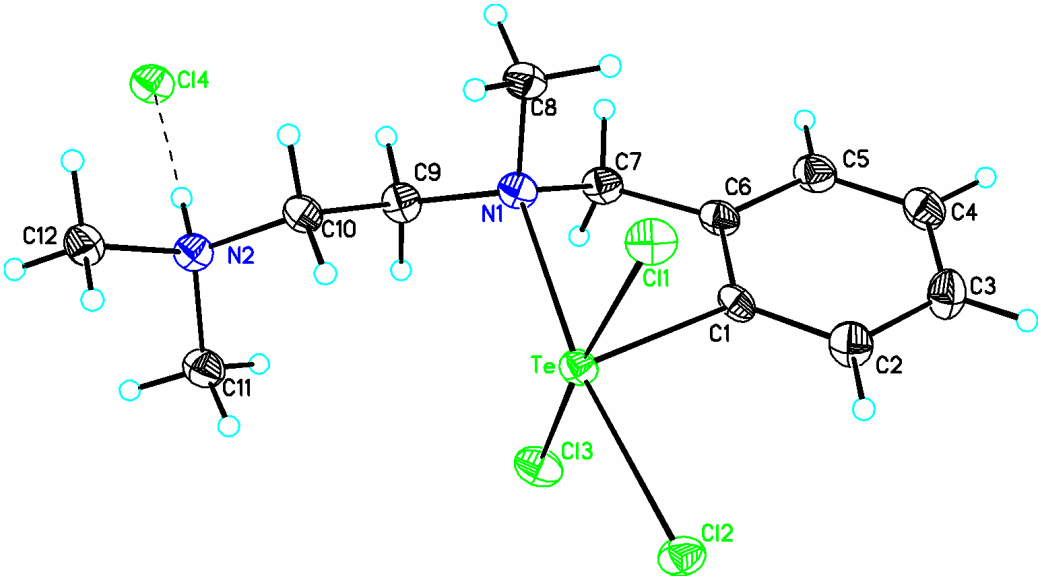

Fig. 2 Molecular structure of **29a** showing 50% probability displacement ellipsoids and the atom numbering scheme. Selected bond distances (Å) and angles (°) are shown in Table 2.

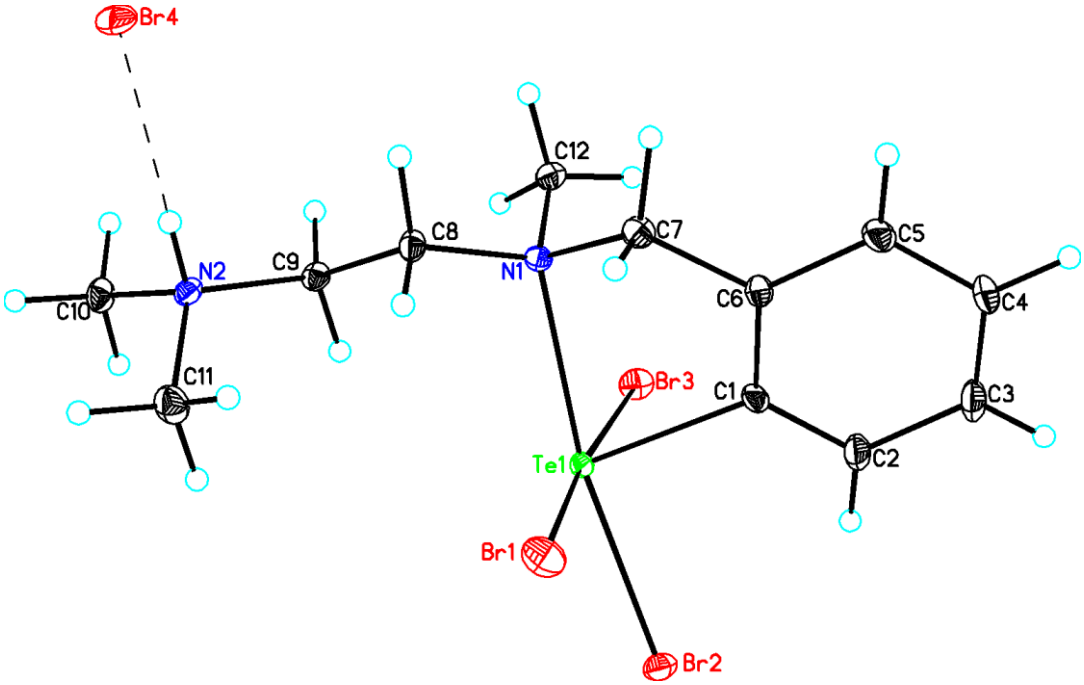

Fig. 3 Molecular structure of **30a** showing 50% probability displacement ellipsoids and the atom numbering scheme. Selected bond distances (Å) and angles (°) are shown in Table 2.

Table 2: Comparison of the experimentally obtained structural parameters (bond distances and bond angles) with that computed for compounds **28a**, **29a**, and **30a**.[a]

	28a			**29a**			**30a**		
		Exp.	Calc		Exp.	Calc.		Exp.	Calc.
Bond distances (Å)	C1−Te	2.145(17)	2.148	C1–Te	2.114(5)	2.131	C1–Te	2.122(5)	2.139
	Te − I1	2.8564(15)	2.959	Te – Cl1	2.5267(13)	2.639	Te – Br1	2.6493(7)	2.888
				Te – Cl2	2.4496(13)	2.580	Te – Br2	2.5946(6)	2.754
	N1−Te	2.426(15)	2.570	Te – Cl3	2.4784(14)	2.684	Te – Br3	2.6731(7)	2.836
	H2B···I2	2.428	2.213	N1 − Te	2.437(4)	2.504	N1− Te	2.463(4)	2.553
				N2-H2B ···Cl4	1.998	1.814	N2-H2NA···Br4	2.28(2)	2.004
Bond angles (°)	N1−Te–I1	169.0(3)	171.05	N1–Te − Cl2	169.08(12)	167.76	N1–Te − Br2	170.15(10)	169.18
	C1−Te–I1	94.9(5)	96.96	C1– Te – Cl1	84.69(14)	90.70	C1–Te–Br1	88.94(15)	92.27
			−	C1–Te – Cl2	93.20(15)	92.90	C1–Te – Br2	94.87(15)	95.09
				C1–Te – Cl3	88.52(14)	90.85	C1–Te – Br3	85.18(15)	92.06
				Cl1–Te – Cl3	173.21(5)	171.68	Br1–Te – Br3	173.97(2)	172.30

[a]The optimized geometrical parameters are obtained at the B3LYP level of theory and 6-311+g(d), lanl2dzbasis set.

*3.3.3. Molecular Structures of **31**, **32** and **33***

Organomercury(II) halides **31** (Fig. 4), and **32** (Fig. 5) crystallize in monoclinic crystal system, however, mercury(II) azide **33** (Fig. 6) crystallizes in a triclinic crystal system. Interestingly, in **31** the Hg atom is bonded to both Cl/Br with occupancies of 0.55:0.45 (*vide infra).* All the three organomercury compounds exhibit coordination with both the N atoms and have a non-linear structure rather than the distorted square planar geometry reported for [2-(Me_2NCH_2)C_6H_4]HgCl [44]. The Hg···N distances [Hg···N1/Hg···N2 2.680(4)/2.635(5) Å in **31**, 2.690(6)/2.636(6) Å in **32** and 2.656(5)/2.699(6) Å in **33**] are considerably shorter than the sum of the van der Waals radii for Hg and N [Σr_{vdw} (Hg, N), 3.05 Å] and greater than the sum of the covalent radii for Hg and N[Σr_{cov}(Hg,N), 2.03 Å] [43]. The C-Hg-X (X = Cl, Br, N(11)) bond angles for **31**, **32** and **33** are deviated from the linear geometry with bond angles of 167.8(7)°, 168.1(2)° and 172.6(3)°, respectively. The angle observed in **33** is smaller than the reported

value in [2-(Me_2NCH_2)C_6H_4]HgN_3 (175.3(2)° [45]. The deviation in C-Hg-Cl/Br bond angle is close to that reported for pentafluorophenylmercury chloride when it forms complexes with both DMSO and DMF, 169.7(2)°[46]. It is clearly evident that the higher deviation of C-Hg-X [X = Cl, Br, N(11)] bond angle is due to the stronger coordination of the both the amine nitrogen atoms to mercury. The covalent nature of the azide is indicated by N3-N4 (1.096(9) Å) bond length, which is shorter than N4-N5 1.173(9) Å bond distance. The covalent azide **33** shows a bent *trans* configuration with an N3-N4-N5 bond angle of 172.9(9)°. The bent unit has different N-N bond lengths. One of these bonds of azide *i.e.* (N3-N4) is found to be significantly shorter than a typical N-N single bond (1.44 Å), while the other bond (N4-N5) is slightly longer than the N≡N triple bond (1.098 Å). The Hg···N(1) bond length in **33** is 2.656(6) Å and is close to those reported by Klapötke *et al.*[47]. The packing diagram reveals the presence of a weak intermolecular metallophilic interaction (Hg···Hg) between two Hg atoms in crystal lattices of **33**, [3.940(5)] Å (Fig. S48 see Supporting Information pageS46). The distance of 3.940(5) Å is slightly smaller than the sum of the van der Waals radii for Hg···Hg (Σr_{vdw}= 3.96 Å) [43c]. These intermolecular interactions are longer than the Hg···Hg distances reported for [{2,6-(Me_2NCH_2)$_2$(*p*-*t*-Bu)C_6H_2]HgN_3 (3.92Å)[45].

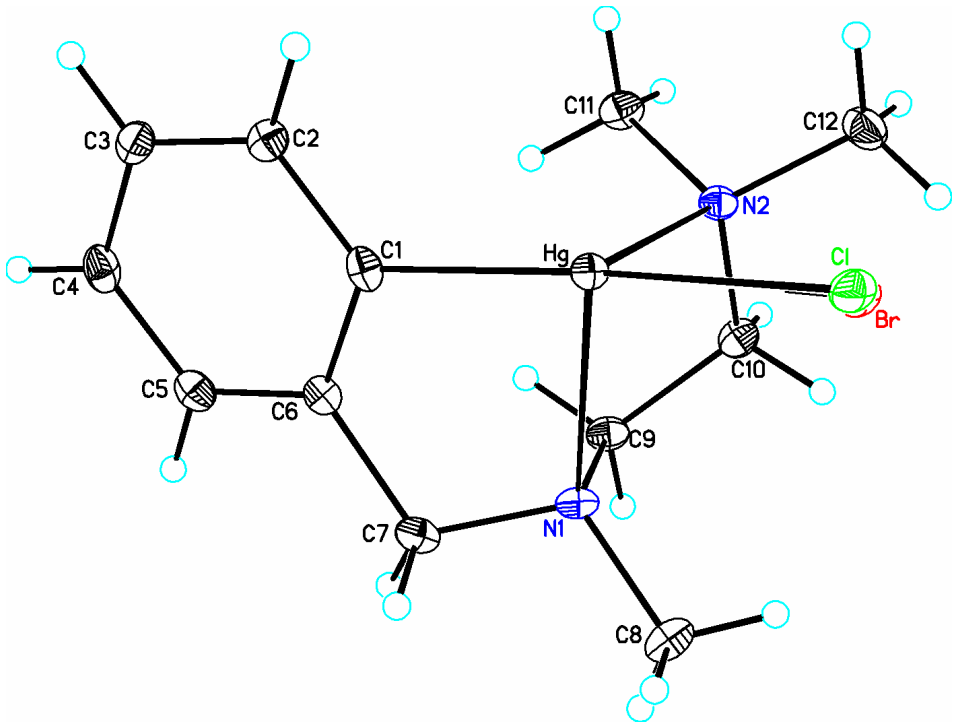

Fig. 4 Molecular structure of **31** showing 50% probability displacement ellipsoids and the atom numbering scheme. Selected bond distances (Å) and angles (°) are shown in Table 3.

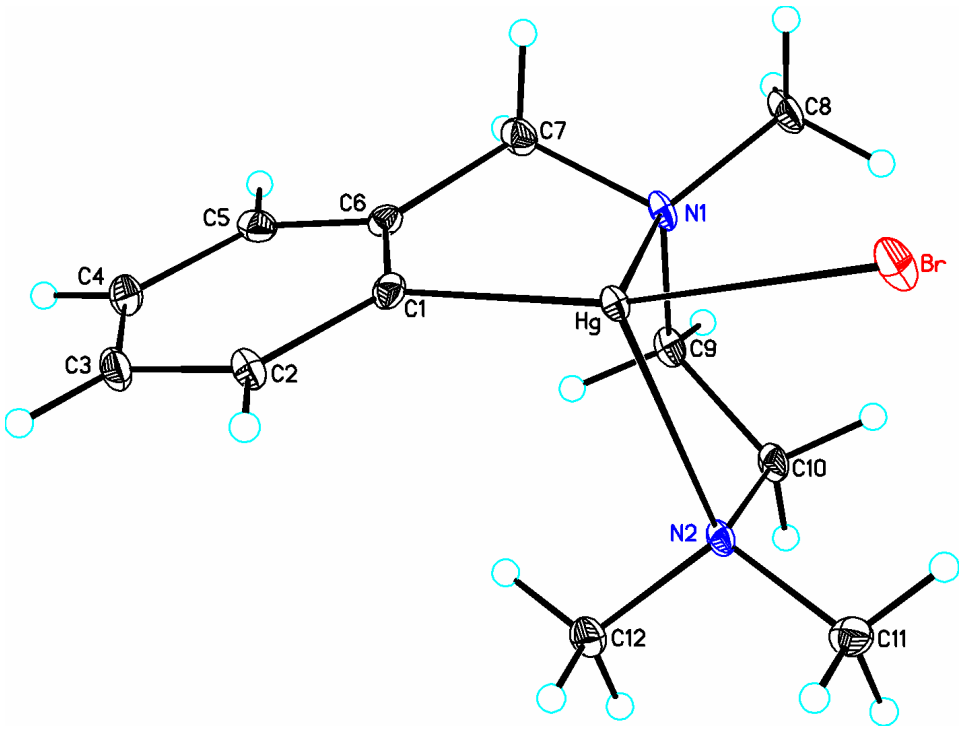

Fig. 5 Molecular structure of **32** showing 50% probability displacement ellipsoids and the atom numbering scheme. Selected bond distances (Å) and angles (°) are shown in Table 3.

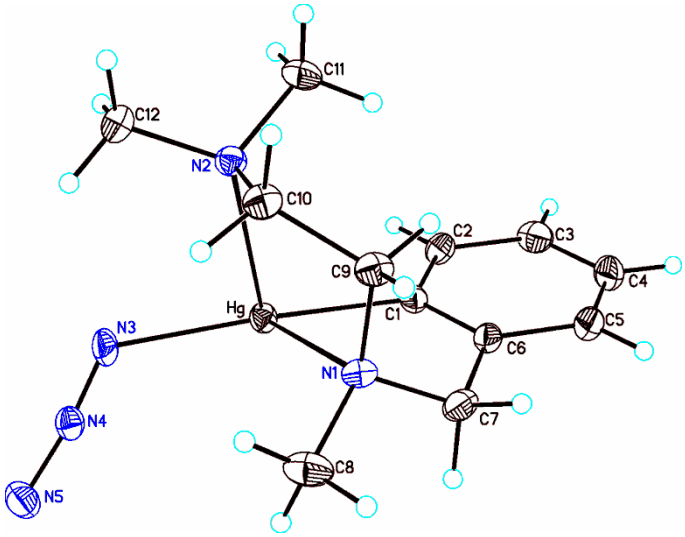

Fig. 6 Molecular structure of **33** showing 50% probability displacement ellipsoids and the atom numbering scheme. Selected bond distances (Å) and angles (°) are shown in Table 3.

Table 3: Comparison of the experimentally obtained structural parameters (bond distances and bond angles) with that computed for compounds **31**, **32** and **33**[a]

	31			**32**			**33**		
		Exp.	Calc.		Exp.	Calc.		Exp.	Calc.
Bond Distances Å)	C1−Hg	2.078(5)	2.230	C1−Hg	2.068(7)	2.240	C1−Hg	2.062(7)	2.224
	Hg−Cl	2.4164(15)	2.525	Hg−Br	2.467(8)	2.657	N1−Hg	2.656(6)	2.728
	N1−Hg	2.680(4)	2.728	N1−Hg	2.690(6)	2.734	N2−Hg	2.699(6)	2.800
	N2−Hg	2.635(5)	2.797	N2−Hg	2.636(6)	2.812	N3−Hg	2.108(6)	2.237
Bond Angles (°)	C1−Hg−Cl	167.8(7)	166.77	C1−Hg−Br	168.1(2)	165.77	C1−Hg−N3	172.6(3)	173.21
	N1−Hg−N2	70.22(13)	69.21	N1−Hg−N2	70.72(18)	68.88	N1−Hg−N2	69.52(17)	69.16

[a]The optimized geometrical parameters are obtained at the B3LYP level of theory and 6-311+g(d), lanl2dz basis set.

3.4. DFT Calculations

In order to gain insight into the structure and nature of bonding in the synthesized organotellurium and organomercury compounds, DFT calculations were carried out. The optimized geometries of the compounds **28-33** showed good agreement with experimentally determined X-ray crystal structures. A comparison of the experimentally obtained structural parameters (bond distances and bond angles) with the bond parameters of optimized geometries is shown in Table 2 and Table 3. To examine whether the coordination mode of N donor atoms can be a contributing factor in obtaining organotellurium compounds as salts, we investigated the coordination mode of potentially tridentate, *cis*-pincer (N1,N2,C) ligand with Te. For this purpose, we optimized the geometries of unprotonated forms of **28a**, **29a** and **30a** with the nitrogen atoms directed towards Te for possible coordination), which have been represented as **28**, **29** and **30**, respectively. The optimized geometries with corresponding Te···N distances are shown in Fig. S49. The optimized geometries revealed that the terminal N2 atoms do not involve in strong coordination with Te. For instance, in **28**, the terminal N2 has Te···N2 distance of 3.669 Å, which is larger than sum of van der Waals radii of Te and N (3.61 Å) and thus, does not coordinate with Te. Further, in **29** and **30**, the terminal N2 atoms coordinate very weakly with Te. The Te···N2 bond distance and its Wiberg bond index in **29** are 3.046 Å and 0.076, respectively, while the Te···N1 bond distance is very short (2.514 Å), with very a high Wiberg bond index of 0.263. This indicates a preferential coordination of Te with N1 over terminal N2 donor atom. The coordination of terminal N2 with Te in organotellurium compounds is so weak that the secondary bonding interaction energy for the Te···N1 interaction is more than 7 times (44.1 kcal/mol for **29** and 40.8 kcal/mol for

30, see Fig. S50) as large as for the Te···N2 interaction ($E_{Te\cdots N2}$ is 6.5 kcal/mol in **29** and $E_{Te\cdots N2}$ is 5.8 kcal/mol in **30**, see Fig S50**).** This is probably due to formation of very stable T-shaped/ trigonal bipyramidal geometry around central Te with 3c-4e (N-Te-X) bond. Compound **27** is 10-Te-3 system whereas **29** and **30** are 12-Te-5 system, instead of 12-Te-4/14-Te-6 systems which would have formed with the coordination of N2 [48]. The hydrolysis of **28,** having weakly acidic TeI group, even with traces of water is probably facilitated by no coordination/very weak coordination of N2 with Te in **29-30**. In a way, N2 acts as a proton sponge. Unlike organotellurium compounds, in organomercury derivatives (**31-33**) both the donor N atoms of ligand coordinate to Hg with equivalent ease (as evident from the similar Hg-N1 and Hg-N2 bond distances and WBI indices in Table S1) and thereby have both the nitrogen atoms coordinated to Hg.

The nature of M···N (M = Te, Hg) interaction in **28a, 29a, 30a 31, 32 and 33** was studied with the aid of Natural Bond Orbital (NBO) analysis (Fig. 7). It has been earlier reported in literature that Te/Se···N/O interactions can include both electrostatic as well covalent contributions [49,50]. We have calculated the electrostatic interaction (E_{el}) energy for Te···N interaction from their respective atomic charges assuming a point charge model. The net atomic charges on Te and N in **28a-30a** calculated by the natural population analysis (NPA) are shown in Table S2 (see Supporting Information, page S49). The NPA negative charges on N and positive charges on Te atoms clearly show the significance of electrostatic interaction between them. The calculated electrostatic interaction energy of 108.5 kcal/mol and 87.0 kcal/mol for Te···N interaction in Te(IV) compounds **29a** and **30a** was at least twice as compared with E_{el} of 35.8 kcal/mol for Te(II)···N interaction in **28a**. This is clearly due to the higher net positive NPA charge on

Te(IV). Moreover, the higher value of E_{el} in **29a** as compared with **30a** is due to the high electronegativity of the Cl atom attached to Te in **29a**. The covalent contribution for the Te···N interaction was determined using NBO second order perturbation energies. The NBO second order perturbation energies $E_{NBO(Te\cdots N)}$ for **28a**, **29a** and **30a** were 30.9, 44.1 and 39.2 kcal/mol, respectively. The origin of this interaction is due to the donation of electron density from the lone pair of electrons on N (lp(N)) to the antibonding orbital of Te-X bond (σ*(Te-X)) i.elp(N) →σ*(Te-X) interaction. The Wiberg bond indices (WBI) for the Te···N interaction are displayed in Table S1. Among the organotellurium compounds, it is lowest for **28a** (0.212) and highest for **29a** (0.278). This is in line with the shortest Te···N distance of 2.504 Å and highest $E_{NBO(Te\cdots N)}$ interaction energy of 44.1 kcal/mol for **29a.** For organomercury compounds (**31**-**33**) the electrostatic energy contribution for the Hg···N interactions is significant, which ranged from 68.9-84.0 kcal/mol. The second order perturbation energies {$E_{NBO(Hg\cdots N)}$} from NBO analysis revealed that the Hg···N interaction arise from orbital interaction between lp(N) →σ*(Hg-C) orbital as well from lp(N)→lp*(Hg) orbital interaction and $E_{NBO(Hg\cdots N)}$ varies from 8.1-12.5 kcal/mol.

The nature of N···Te and Hg···N interaction in **28a, 29a, 30a 31, 32** and **33** was also studied from a topological point of view with the help of Atoms in Molecules analysis. The important parameters obtained from the AIM calculation for the Te···N and Hg···N interaction are listed in Table S2. The presence of a bond critical point (bcp) for Te···N and Hg···N interaction clearly showed the existence of Te···N and Hg···N interactions. In the case of organotellurium compounds, the electron density for the Te···N interaction $\rho_{(Te\cdots N)}$ varied from 0.044-0.054 a.u (Table S2). The positive values of Laplacian of

electron density ($\nabla^2\rho_{Te\cdots N}$) at the bcp, suggests a dominant electrostatic character for the Te···N interaction. The negative values of local energy density ($H_{Te\cdots N}$) point toward covalent character of Te···N interaction, however, the relatively lower magnitude of $H_{Te\cdots N}$ signifies dominant electrostatic contribution to the Te···N interaction. For the organomercury compounds **31-33**, the values of electron density for the weak Hg···N interactions lies in the range of 0.025-0.030 a.u. The positive values of Laplacian of electron density ($\nabla^2\rho_{Hg\cdots N}$) and relatively low values of local energy density ($H_{Hg\cdots N}$) at the bcp suggest a dominant electrostatic character for the Hg···N interaction. In addition, for compound **33**, which possess a Hg-N(azide) bond, the electron density at bcp for this bond is relatively high with a value of 0.074 a.u. Also, the large and negative value of $H_{Hg\text{-}N}$(-0.0166 a.u) clearly suggests a dominant covalent character for the Hg-N azide bond.

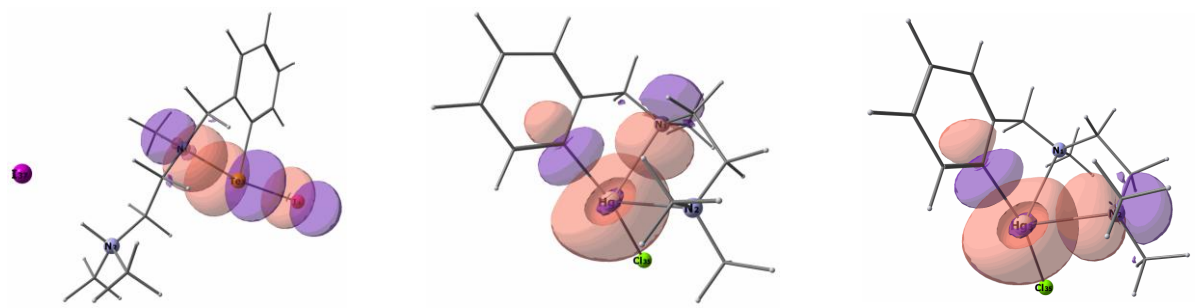

(a) **(b)** **(c)**

Fig. 7 NBO overlap diagram for (a) for lp(N) →σ*(Te-I) donor-acceptor interaction in **28a** and (b,c) lp(N) →σ*(Hg-C) donor-acceptor interactions for both the N1 and N2 atoms in **31.**

4. Conclusions

In conclusion, a series of organochalcogenides derived from *cis*-pincer C,N,N'-chelating aryldiamine ligand has been synthesized and characterized by multinuclear NMR and X-ray single crystal structure analysis. Single crystal structural studies on several tellurium trihalides showed that one of the N atom strongly coordinates with the tellurium atom as the Te···N distances are significantly shorter than the sum of their van der Waals radii, however, terminal nitrogen does not show any intramolecular Te···N interaction. Instead, terminal nitrogen is protonated in all the structurally characterized organotellurium halides in our study. On the other hand, organomercury compounds, which were obtained under similar reaction conditions, show strong Hg···N interactions with both the nitrogen atoms. Also, in contrast to the organotellurium halides, terminal nitrogen does not show any protonation in the case organomercury halides.

Acknowledgements

H.B.S. is grateful to the Department of Science and Technology (DST), J. C. Bose Fellowship, New Delhi, for funding. P.S. thanks Science and Engineering Research Board (SERB), New Delhi for a Start-Up Research Grant for Young Scientist (SB/FT/CS-036/2012).

Appendix A. Supplementary data

Supplementary data associated with this article can be found, in the online version, at http://dx.doi.org/xxxxxxxx.

References

[1] M.A.W. Lawrence, K.-A. Green, P.N. Nelson, S.C. Lorraine, Polyhedron 143 (2018) 11–27. (b) G. vanKoten, Organometallics 31 (2012) 7634–7646. (c) N. Selander, K.J. Szabó, Chem. Rev. 111 (2011) 2048–2076.

[2] J. Choi, A.H.R. MacArthur, M. Brookhart, A.S. Goldman, Chem. Rev. 111 (2011) 1761–1779.

[3] (a) R. Jambor, L. Dostal, The Chemistry of Pincer Complexes of 13–15 Main Group Elements. In: G. van Koten, D. Milstein D. (eds) Organometallic Pincer Chemistry. Topics in Organometallic Chemistry, **40**. Springer, Berlin, Heidelberg 2013. (b) B. Glowacki, M. Lutter, H. Alnasr, R. Seymen, W. Hiller, K. Jurkschat, Inorg. Chem. 56 (2017) 4937–4949. (c) B. Nayyar, R. Kapoor, M. Lutter, H. Alnasr, K. Jurkschat, Eur. J. Inorg. Chem. 33 (2017) 3967–3978.

[4] (a) V.A. Benin, J.C. Martin, M.R. Willcou, Tetrahedron 53 (1997) 10133–10154. (b) A.P. Singh, H.W. Roesky, E. Carl, D. Stalke, J.-P. Demers, A. Lange, J. Am. Chem. Soc. 134 (2012) 4998–5003. (c) M. Wagner, T. Zçöler, W. Hiller, M.H. Prosenc, K. Jurkschat, Chem. Eur. J. 19 (2013) 9463–9467.

[5] H. Fujihara, H. Mima, N. Furukawa, J. Am. Chem. Soc.117 (1995) 10153–10154.

[6] K. Kobayashi, S. Sato, E. Horn, N. Furukawa, Z. Kristallogr. NCS 215 (2000) 21–22.

[7] A. Beleaga, V.R. Bojan, A. Pöllnitz, C.I. Raţ, C. Silvestru, Dalton Trans. 40 (2011) 8830–8838.

[8] A. Pop, A. Silvestru, E.J. Juárez-Pérez, M. Arca, V. Lippolis, C. Silvestru, Dalton Trans. 43 (2014) 2221–2223.

[9] R.A. Varga, M. Kulcsar, A. Silvestru, Acta Cryst. E66, (2010) o771.

[10] A. Gupta, H.B. Singh, R.J. Butcher, IUCR Data 2 (2017) x171634.

[11] B. Kersting, M. DeLion, Z. Naturforsch. 54b (1999) 1042–1047.

[12] S.S. Zade, S. Panda, S.K. Tripathi, H.B. Singh, G. Wolmershäuser, Eur. J. Org. Chem. (2004) 3857–3864.

[13] (a) A. Welter, L. Christiaens, W.-P. Ferdinand, Eur. Pat. Appl. EP 44453 (1982) Chem. Abstr., 96 (1982) 199699v. (b) L. Engman, A. Hallberg, J. Org. Chem. 54 (1989) 2964–2996. (c) A. Müller, E.Cadenas, P. Graf, H. Sies, *Biochem. Pharmacol.* 33 (1984) 3235–3239.(b)A. Wendel, M.Fausel, H.Safayhi, G. Tiegs, R. Otter, Biochem. Pharmacol. 33 (1984) 3241–3245. (c) T. Schewe,Gen. Pharmacol. 26 (1995) 1153–1169.

[14] K. Selvakumar, H.B. Singh, N. Goel, U.P. Singh, Organometallics 30 (2011) 3892–3896.

[15] K. Selvakumar, H.B. Singh, To be published.

[16] (a) M.H.P. Rietveld, I.C.M. W.-Ooyevaar, G.M. Kapteijn, D.M. Grove, W.J.J. Smeets, H. Kooijman, A.L. Spek, G. van Koten, Organometallics 13 (1994) 3782–3787. (b) A.M. Arink, C.M.P. Kronenburg, J.T.B.H. Jastrzebski, M. Lutz, A.L. Spek, R.A. Gossage, G. van Koten, J. Am. Chem. Soc.126 (2004) 16249–16258.

[17] R. Rippstein, G. Kickelbick, U. Schubert, Inorg. Chim. Acta 290 (1999), 100–104.

[18] D. Bhowmick, G. Mugesh, Org. Biomol. Chem. 13 (2015) 9072–9082.

[19] (a) G. Reeske, A.H. Cowley, Chem. Commun., (2006) 4856–4858. (b) C.D. Martin, P.J. Ragogna, Inorg. Chem. 51(2012) 2947–2953.

[20] J.G. Donkervoort, C.M.P. Kronenburg, B.–J. Deelman, J.T.B.H. Jastrzebski, N. Veldman, A.L. Spek, G. van Koten, J. Organomet. Chem. 547 (1997) 349–355.

[21] M.H.P. Rietveld, W. Teunissen, H. Hagen, L. van de Water, D.M. Grove, P.A. van der Schaaf, A. Mühlebach, H. Kooijman, W.J.J. Smeets, N. Veldman, A.L. Spek, G. van Koten, Organometallics 16 (1997) 1674–1684.

[22] T.G. Richmond, Coord. Chem. Rev.105 (1990) 221–250. (b) B.P. Buffin, A.M. Arif, T.G. Richmond, J. Chem. Soc. Chem. Commun. (1993) 1432–1434. (c) B.P. Buffin, M.J. Poss, A.M. Arif, T. G. Richmond, Inorg. Chem. 32 (1993) 3805–3806.

[23] (a) E.G. Bowes, S. Pal, J.A. Love, J. Am. Chem. Soc. 137 (2015) 16004–16007. (b) I.C.M. W.-Ooyevaar, G.M. Kapteijn, D.M. Grove, W.J.J. Smeets, A. L. Spek, G. van Koten, J. Chem. Soc., Dalton Trans. (1994) 703–711.

[24] R.M. Ceder, J. Granell, G. Muller, G. Organometallics 15 (1996) 4618–4624.

[25] (a) P.L. Alster, J. Boersma, G. van Koten, Organometallics 12 (1993) 1629–1638. (b) P.L. Alsters, P.F. Engel, M.P. Hogerheide, M. Copijn, A.L. Spek, G. van Koten, Organometallics 12(1993) 1831–1844.

[26] C.M.P. Kronenburg, J.T.B.H. Jastrzebski, J. Boersma, M. Lutz, A.L. Spek, G. van Koten, J. Am. Chem. Soc. 124 (2002) 11675–11683.

[27] G. Brauer, Handbook of Preparative Inorganic Chemistry, 3rd ed; Academic Press: New York, 1975.

[28] O. Foss, Inorg. Synth. 4 (1953) p 88.

[29] G.M. Sheldrick, Acta Cryst. A64 (2008), 112-122.

[30] D.T. Cromer, J.T. Waber, International Tables for X-ray Crystallography, Kynoch Press, Birmingham, U.K, 1974.

[31] M.J. Frisch, G.W. Trucks, H.B. Schlegel, G.E. Scuseria, M.A. Robb, J.R. Cheeseman, G. Scalmani, V. Barone, B. Mennucci, G.A. Petersson, H. Nakatsuji, M. Caricato, X. Li, H.P. Hratchian, A.F. Izmaylov, J. Bloino, G. Zheng, J.L. Sonnenberg, M. Hada, M. Ehara, K. Toyota, R. Fukuda, J. Hasegawa, M. Ishida, T. Nakajima, Y. Honda, O. Kitao, H. Nakai, T. Vreven, J.A. Montgomery, Jr., J.E. Peralta, F. Ogliaro, M. Bearpark, J.J. Heyd, E. Brothers, K.N. Kudin, V.N. Staroverov, R. Kobayashi, J. Normand, K. Raghavachari, A. Rendell, J.C. Burant, S.S. Iyengar, J. Tomasi, M. Cossi, N. Rega, J.M. Millam, M. Klene, J.E. Knox, J.B. Cross, V. Bakken, C. Adamo, J. Jaramillo, R. Gomperts, R.E. Stratmann, O. Yazyev, A.J. Austin, R. Cammi, C. Pomelli, J.W. Ochterski, R.L. Martin, K.Morokuma, V. G. Zakrzewski, G.A. Voth, P. Salvador, J.J. Dannenberg, S. Dapprich, A.D. Daniels, Ö. Farkas, J.B. Foresman, J.V. Ortiz, J. Cioslowski, D.J. Fox, Gaussian 09, RevisionA.02, Gaussian, Inc., Wallingford, CT, 2009.

[32] (a) A.D. Becke, Phys. Rev. A, 38 (1988) 3098–3100. (b) A.D. Becke, J. Chem. Phys. 98 (1993) 5648–5662. (c) C. Lee, W. Yang, R.G. Parr, Phys. Rev. B Condens. Matter 37 (1988) 785–789.

[33] (a) A.E. Reed, L.A. Curtiss, F. Weinhold, Chem. Rev. 88 (1988) 899–926. (b) E.D. Glendening, J.E. Reed, J.E. Carpenter, F. Weinhold, Natural Bond Orbital (NBO) Version 3.1.

[34] R.F.W. Bader, Atoms in Molecules: A Quantum Theory, Clarendon Press, Oxford, 1990.

[35] T. Lu, F. Chen, J. Comput. Chem. 33 (2012) 580–592.

[36] D.A. Zhurko, G.A. Zhurko, ChemCraft (version 1.8), 2018, Available at http://www.chemcraftprog.com.

[37] P. Singh, H.B. Singh, R.J. Butcher, Acta Cryst. E74(2018) 1151–1154.

[38] A. Gupta, H.B. Singh, R.J. Butcher, Acta Cryst. E73(2017) 1679–1682.

[39] (a) M. Baiwir, G. Llabres, O. Dideberg, L. Dupont, J.L. Piette, Acta Cryst. B30 (1974) 139–143. (b) I.D. Sadekov, A.A. Maksimenko, A.V. Zakharov, B.B. Rivkin, Chem. Heterocycl. Compd. 30 (1994) 243–253.

[40] K. Ouyang, W. Hao, W.-X. Zhang, Z. Xi, Chem. Rev. 115 (2015) 12045–12090.

[41] H. Duddeck, Prog. in NMR Spectrosc. 27 (1995) 1–323.

[42] B. Wrackmeyer, R. Contreras, Annu. Rep. NMR Spectrosc. 24 (1992) p267.

[43] (a) J. Emsley, Die Element, Walter de Gruyter, Berlin, 1994. (b) N. Wiberg, Holleman-Wiberg- Lehrbuch der AnorganischenChemieWalter de Gruyter, Berlin, 1994. (c) A.J. Bondi, Phys. Chem. 68 (1964) 441–451.

[44] O. Bumbu, C. Silvestru, M.C. Gimeno, A. laguna, J. Organomet. Chem. 689 (2004) 1172–1179.

[45] S. Das, H.B. Singh, R.J. Butcher, J. Organomet. Chem. 799–800 (2015) 184–194.

[46] M. Tschinkl, A. Schier, J. Riede, F.P. Gabbaï, Organometallics 18(1999) 2040–2042.

[47] T.M. Klapötke, B. Krumm, R. Moll, Z. Anorg. Allg. Chem. 637 (2011) 507–514.

[48] C.W. Perkins, J.C. Martin, A.J. Arduengo III, W. Lau, A. Alegria, J.K. Kochi, J. Am. Chem. Soc.102 (1980) 7753–7759.

[49] (a) H. Yang, T.P. Lin, F.P. Gabbaï, Organometallics 33(2014) 4368–4373. (b) R.B. Sunoj, Theoretical aspects of organoselenium chemistry, in: Z. Rappoport (Ed.),

PATAI'S chemistry of functional groups, Wiely, Chichester, 2011, (c) R.L. Longo, P.H. Menezes, Theoretical and computational aspects of organotellurium compounds, in : Z. Rappoport (Ed.), PATAI'Schemistry of functional groups, Wiely, Chichester, 2011.

[50] (a) M. Iwaoka, S. Tomoda, J. Am. Chem. Soc. 118 (1996) 8077–8084. (b) M. Iwaoka, T. Katsuda, H. Komatsu, S. Tomoda, J. Org. Chem. 70 (2005) 321–327. (c) M. Iwaoka, H. Komatsu, T. Katsuda, S. Tomoda, J. Am. Chem. Soc. 126 (2004) 5309–5317. (d) S.K. Tripathi, U. Patel, D. Roy, R.B. Sunoj, H.B. Singh, G. Wolmershäuser, R.J. Butcher, J. Org. Chem. 70 (2005) 9237–9247. (e) D. Roy, C. Patel, J.F. Liebman, R.B. Sunoj, J. Phys. Chem. A 112 (2008) 8797–8803.

HIGHLIGHTS

- first examples of organotellurium and -mercury derivatives of a *cis*-pincer substrate.
- computational studies to rationalize the facile protonation of N of terminal amine group and found that either it doesn't coordinate at all with Te or the coordination is very weak.
- terminal amine group of organomercury compounds is not protonated under similar conditions and both the N atoms are weakly coordinated with Hg
- crystal structures of organotellurium and mercury derivatives revealed the presence of characteristic intramolecular N···M, (M = Te, Hg) secondary bonding interactions (SBIs).

GRAPHICS: